Proceedings World Geothermal Congress 2000
Kyushu - Tohoku, Japan, May 28 - June 10, 2000

CHARACTERIZATION OF SMECTITE SCALE AND SCALE INHIBITION TEST BY pH CONTROL AT THE MORI GEOTHERMAL POWER PLANT, JAPAN.

Kaichiro Kasai[1], Keiji Sato[1], So-ichiro Kimura[1], Nobuhiko Shakunaga[2] and Kosei Obara[2]
[1]JMC Geothermal Engineering Co., Ltd.(Geo-E), 72 Sasamori, Ukai, Takizawa-mura, Iwate, 020-0172 JAPAN
[2]Japan Metals & Chemicals Co., Ltd. (JMC), 1-3-6 Saien, Morioka, Iwate, 020-0024 JAPAN

Key Words: smectite, stevensite, scale inhibition, pH control, Mori

ABSTRACT

Smectite scaling became a problem in 1988 at the Mori geothermal power plant, in the well discharges due to an incursion of Mg-rich and low enthalpy fluids. Bulk scale is mainly composed of smectite, plus lesser amorphous silica and calcite. This smectite is identified as stevensite by X-ray diffraction and chemical analysis (mainly MgO and SiO_2, and selectively concentrated MnO). The characteristics and amount of scale of each production line is different depending on its fluid chemistry. Smectite scale is widely distributed in surface pipelines and installations, but its crystallinity decreases toward the re-injection well. Mineral-water equilibrium showed that major factors controlling smectite saturation were an increase of pH by degassing of CO_2 and H_2S, and concentration of solutes, as a result of boiling in the well. Field tests from 1994 to 1996 have been conducted to evaluate pH control methods for inhibiting smectite scaling. As a result, a smectite scale was inhibited by keeping pH at less than 6.5 at the Mori geothermal power plant.

1. INTRODUCTION

The Mori geothermal field is a liquid dominated geothermal field located at the Nigorikawa basin in Southwest Hokkaido, Japan. The Mori geothermal power station of 50 MWe, incorporating a double flash system, has been in operation since 1982 by Hokkaido Electric Power Inc. where Dohnan Geothermal Energy Co., Ltd. (DGE), a subsidiary of Japan Metals & Chemicals Co., Ltd., is a steam supplier.

Nigorikawa basin is a caldera that formed 12,000 years ago. The geothermal system is hosted in Quaternary caldera-fill deposits and Tertiary formations of Pliocene to Miocene age (e.g., Sato, 1988; Ando *et al.*, 1992; Kurozumi and Doi, 1995). The geothermal fluid is formed by simple mixing of heated meteoric water with deep hot aquifer water (around 300^{O}C). The latter has a large component of magmatic and/or altered sea water (Yoshida, 1991). Most of the fluids are produced from a fracture network in the caldera at temperature of 220-260^{O}C. Reservoir fluid is saturated with calcite, resulting in $CaCO_3$ scale deposition in production wells during steam production. However, after application of scale inhibitor (sodium poly-acrylate) began in 1985, the $CaCO_3$ scaling problem was solved.

Stevensite deposition at the Mori geothermal power plant occurred after an abrupt increase of Mg concentration in well discharge in September 1988 (Muramatsu *et al.* 1988; Yoshida, 1991). It is likely that Mg-rich, low enthalpy fluid entered the shallow reservoir as a result of a change in the flow pattern caused by additional drilling. This low enthalpy fluid is estimated to have the same origin as the Nigorikawa hot spring (Yoshida, 1991). Smectite scale causes several problems at the Mori geothermal plant, requiring troublesome and costly elimination every year. This smectite makes it difficult to control operation valves and decreases the capacity of re-injection wells as a result of filling fractures. Similar Mg-rich clay scale has been reported for geothermal systems of Iceland, the Philippines and elsewhere (Gunnlaugsson and Einarsson, 1989; Kristmannsdóttir *et al.*, 1989; Reyes and Cadile, 1989; Hauksson *et al.*, 1995; Beaufort *et al.*, 1995).

2. RESULTS AND DISCUSSION

2.1 Observation and analysis of smectite scale

Field observation

We have observed the state and amount of scale deposited in surface pipelines and installations every year from 1992. Most of the scale is deposited in pipelines of the liquid stream from separators to the re-injection wells. Its maximum thickness is *ca.*20cm at the end manhole. The amount of scale differs in the three lines of the production system (300 line > 200 line > 100 line) depending on the Mg concentration of fluid discharged from the ten production wells that are gathered into these three lines. Generally, the color and hardness of the scale differs depending on the line or its position in the stream. Scales deposited near the production wells are brownish and hard, and glassy in some cases. Scales become more whitish and soft with increasing distance from the production wells. Scales deposited near the re-injection wells are brickle, soft, poorly crystallized, and are gel in some cases.

X-ray diffraction

Results of X-ray diffraction (XRD) analysis of scale are listed in Table 1, and a typical XRD pattern is shown in Fig. 1 with an SEM image. Scale samples are numbered with “P” or “R” to distinguish the position collected as follows: “P” indicates a line upstream from a tank that pools disposal water from the production wells, and “R” indicates a line downstream from the tank to the re-injection wells. Bulk scale is mainly composed of smectite, with small amounts of amorphous silica, calcite and quartz from formation rocks. Brownish and glassy scale collected from the upstream end reveals a relatively sharp smectite peak. Amorphous silica, with a broad peak, is abundant mostly in the scale collected downstream. We compared the half width of a secondary peak (d(020), d(110)) to evaluate the relationship between the degree of structural disorder of smectite and its deposition site (Table 1). Smectite is widely

distributed in surface pipelines and installations, but there is a tendency for the smectite to become more disordered downstream from the production well to the re-injection well.

Chemical analysis

Chemical analysis of scale is listed in Table 2. The chemical composition of scale varies with increasing distance from the production wells and with decreasing temperature of the fluids. A comparison of chemical compositions and $(MgO+MnO)/SiO_2$ molar ratios of smectite scale (Fig. 2) indicates that scale from upstream has higher values of $(MgO+MnO)/SiO_2$ than scale from downstream. Representative structural formulas of smectite from upstream are listed in Table 3, whereas formulas for scales from downstream are difficult to decide, due to their excess SiO_2 contained as amorphous silica. Manganese rich smectite deposits near the production wells. Overall, Al and Mn contents of tri-smectite decrease with increasing distance from the production wells.

2.3 Mechanism of formation for smectite scale

Mg silicate, including stevensite, has low solubility in warm waters at higher pH. Increased temperature and higher pH will enhance the rate of precipitation. The Mori smectite scaling began when Mg concentration increased abruptly (from 1ppm to 7ppm) in well discharge in September 1988. We hypothesize that formation of stevensite is initiated by mixing Mg-rich and low-enthalpy fluid from shallow wells with SiO_2-rich, high-enthalpy fluid from deep wells, causing the reaction shown in equation (1). This low enthalpy fluid is thought to have been of the Nigorikawa hot spring.

$$3Mg^{2+} + 4H_4SiO_2 \Leftrightarrow Mg_3Si_4O_{10}(OH)_2 + 6H^+ + 4H_2O \quad (1)$$

We calculated the solubility of talc and chrysotile, instead of stevensite, by a chemical simulator, SOLVEQ (Reed, 1998). The Mori water composition is given by Yoshida (1991). Talc and chrysotile are chosen for calculations because their thermodynamic properties are known, whereas no data are available for stevensite and saponite. Analysis of mineral solubility shows that there is a danger of precipitation of Mg silicate from waters after steam separation, where their pH is slightly alkaline in a pipeline, although Mg silicates are undersaturated in the Mori reservoir (Fig. 3). The high temperature smectites are authegenetic minerals that crystallized in response to abrupt supersaturation of the liquid phase during boiling.

Although kinetics of scale deposition can neither be calculated, nor predicted accurately, they are generally influenced by extent of mineral supersaturation, turbulence, smoothness of pipeline, and abundance of suspended material in the liquid, which can act as crystallization nuclei.

2.4 Efficiency of pH control for scale inhibition

We evaluated the potential of pH control to inhibit precipitation of Mg silicate by simulating its solubility at pH values of 5.0, 6.0 and 7.0 at 100 and 150^{O}C by SOLVEQ (shown by a solid square in Fig. 3). It is evident that Mg silicates like chrysotile and talc are undersaturated at slightly acidic conditions of pH 5.0 and 6.0, because the formation reaction of Mg silicate is enhanced to reverse direction as a consequent of H^+ increase, according to equation (1). Therefore, we decided to evaluate the efficiency of pH control for scale inhibition by a field test with a pilot plant at the Mori geothermal field.

2.5 Field test of pH control to inhibit scale formation

We conducted the field tests to evaluate pH control as a scale inhibitor with a test plant (Fig. 4) from 1994 to 1996. The test plant was composed of three lines (A, B, C). The pH in lines A and B were controlled to 7.0, 6.5, 6.0 and 5.0 at room temperature by addition of hydrochloric acid (1%), and line C was a reference with no treatment (natural pH). The testing fluid was fed from 300 line, which has high potential for scaling compared with other two lines (see above). We monitored the pH of liquid samples at room temperature after cooling and condensing two-phase fluids from each test line. After one month and three months of the test, while monitoring pH, flow rate and fluid chemistry, we measured the thickness of scale and corrosion of material. Field tests were conducted in pipes of 27mm inside diameter x 20cm length, made of SUS316 with a weight of *ca.*450g. The flow rate of each test line is regulated at 2.5 ton/hr, that approximates the fluid speed in a real pipeline. The results of field tests are listed in Table 4, and tested specimens after 28 days are shown in Fig. 5. Brownish white scales deposited at 1.4-1.8 g/day in the reference line of natural pH, and 0.75 g/day in the pH 7.0 line, whereas scarcely any scale deposited in the line of pH < 6.5 during the three months. The pipe specimen at pH 5.0 became blackish in color due to slight corrosion.

We demonstrated the possibility of inhibiting smectite scale by pH control (less than 6.5) at the Mori geothermal power plant. Therefore we decided to control pH between 6.0 and 6.5 in order to inhibit smectite scale while avoiding corrosion. We treated pH of liquid lines downstream from separators with inorganic acid to hold pH at ~ 6.5 for about two years. We succeeded in diminishing the amount of scale.

3. CONCLUSIONS

Smectite scale deposited in liquid lines of the Mori geothermal power plant was identified as stevensite by its XRD pattern and chemical composition. We suppose that stevensite formation is initiated by mixing Mg-rich, low enthalpy fluid from shallow wells with SiO_2-rich, high enthalpy fluid from deep wells.

We were able to inhibit smectite scale by pH control (less than 6.5) as demonstrated in field tests. We conclude that pH control is able to eliminate scale, allowing smooth installation operation and thus stabilizing steam production.

ACKNOWLEDGEMENTS

The authors appreciate JMC for permission to publish

these results. The authors would like to thank DGE plant operators for their kind cooperation in sampling and monitoring for the field test. The authors would like to thank M. H. Reed for his useful suggestion and review of the original manuscript.

REFERNCES

Ando, S., Kurozumi, H. and Komatsu, R. (1992). Structure and Caldera-fill Deposits of Nigorikawa Caldera. *Abstr.*, *29th International Geological Congress*, Vol.2, pp.480.

Beaufort, D., Papapanagiotou, P., Patrier, P., Fujimoto, K. and Kasai, K. (1995). High temperature smectites in active geothermal systems. In: *7th Water-Rock Interaction*, Kharaka and Chudaev (Eds)., Balkema, Rotterdam, pp.493-496.

Gunnlaugsson, E. and Einarsson, A. (1989). Magnesium-silicate scaling in mixture of geothermal water and deaerated fresh water in a district heating system. *Geothermics*, Vol.18, pp.113-120.

Hauksson, T., Porhallsson, S. Gunnlaugsson, E. and Albertsson, A. (1995). Control of Magnesium Silicate Scaling in District Heating Systems. In *Proc. of the World Geothermal Congress*, pp.2487-2490.

Kristmannsdóttir, H., Ólafsson, M. and Thórhallsson, S. (1989). Magnesium silicate scaling in district heating system in Iceland. *Geothermics*, Vol.18, pp.191-198.

Kurozumi, H. and Doi, N.(1995). Inner structure of the funnel-shaped Nigorikawa caldera clarified by 3km deep geothermal wells, Hokkaido, Japan. *IUGG XXI General Assembly Abstracts,* B419.

Muramatsu, Y., Kano, S. and Kitamura, T. (1988). Formation of tetrahederite from geothermal fluid at wells of the Nigorikawa geothermal field, southern Hokkaido. *J. Mineral. Soc. Japan*, Vol.18, pp.301-310 (in Japanese with English abstract).

Reyes, A. G. and Cadile, C. M. (1989). Characterization of clay scales forming in Philippine geothermal wells. *Geothermics*, Vol.18, pp.429-446.

Sato, K. (1988). Mori Geothermal Power Plant. *Proc. of Int. Sym. on Geothermal Energy, Kumamoto and Beppu, Japan*, pp.21-25.

Reed, M. H. (1998). Calculation of simultaneous chemical equilibria in aqueous-mineral-gas systems and its application to modeling hydrothermal processes. In: *Techniques in Hydrothermal Ore Deposits Geology*, J. Richards and P. Larson (Eds)., Reviews in Economic Geology, Vol.10, pp.109-124.

Yoshida, Y. (1991). Geochemistry of the Nigorikawa Geothermal System, southeast Hokkaido, Japan. *Geochemical Journal*, Vol.25, pp.203-222.

Table 1a . Mineralogy of scales identified by XRD analysis. Sample obtained at surface installations for steam production (Sample number is 24).

sample	Qtz	Cal	ams	St	half width(°) of XRD peak at 19.6°(=2θ)
P-01B		○		◎	1.35
P-02		○		◎	0.81
P-05A				◎	0.54
P-05B				◎	1.62
P-06A				◎	0.95
P-06B				◎	0.95
P-07A	○	○		◎	1.08
P-08A		○		◎	1.08
P-08B		○		◎	0.81
P-12A				◎	0.95
P-12B		○		◎	1.35
P-12C	○	○		○	0.95
P-13A		○		◎	1.08
P-13C		○		○	0.81
P-13D	○	○		◎	1.08
P-14A		○		◎	1.22
P-14B		○		◎	1.89
P-14C				◎	1.08
P-14D		○		◎	0.95
P-16A				◎	1.08
P-17C			△	◎	1.62
P-18B		○		◎	0.95
P-18C	○	○		◎	1.62
P-21		○		◎	1.08

(Sampling date : 10/Aug/ 93)

Abbreviations correspond to:
Qtz: quartz, Cal: calcite, ams: amorphous silica, St: stevensite
Semi-quantitative classification:
◎: abundance, ○ : medium, △ : rare

Table 1b . Mineralogy of scales identified by XRD analysis. Sample obtained at pipeline from surface installation to re-injection wells (Sample number is 27).

sample	Qtz	Cal	ams	St	half width(°) of XRD peak at 19.6°(=2θ)
R-01A		○		◎	1.62
R-01B		○		◎	1.62
R-01D		○		◎	1.35
R-01F		○		◎	1.08
R-02B			△	◎	1.35
R-05G	○	○		◎	1.22
R-05L		○		◎	1.35
R-06B		○		○	1.35
R-07B		○	△	◎	1.89
R-08				◎	1.62
R-09		○		◎	1.35
R-11A				◎	2.16
R-11A'		○		◎	1.08
R-12A		○		◎	1.35
R-12G			△	△	1.62
R-12K				◎	1.49
R-14		○		◎	1.89
R-16		○		◎	1.35
R-18				◎	1.62
R-20		○		◎	1.35
R-22				◎	1.08
R-24				◎	1.22
R-26				◎	1.35
R-28				◎	1.35
R-30				△	1.08
R-35				◎	1.35
P-37				◎	1.35

(Sampling date : 10/Aug/93)

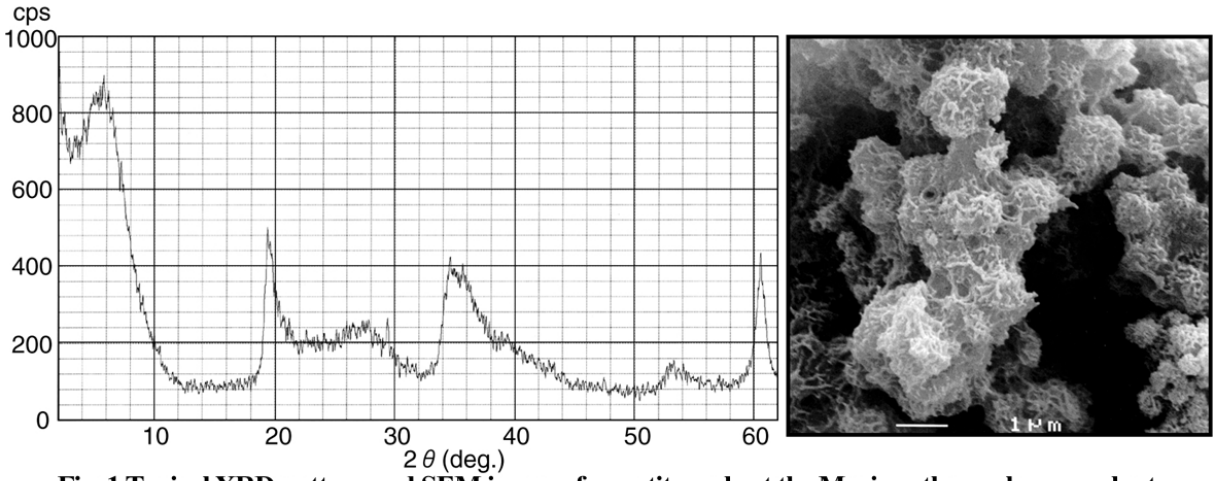

Fig. 1 Typical XRD pattern and SEM image of smectite scale at the Mori geothermal power plant.

Table 2. Chemical composition of scale sample.

(weight %)

Sample	SiO_2	Al_2O_3	FeO	MnO	MgO	CaO	Na_2O	K_2O	$+H_2O$	$-H_2O$	total
P-06A	51.2	1.6	0.1	1.6	23.4	0.6	1.4	0.3	9.1	7.1	96.4
P-06B	45.3	1.9	1.7	9.1	15.9	1.1	1.0	0.3	10.6	10.6	97.5
P-14A	47.1	1.4	0.4	2.9	22.0	0.9	1.4	0.2	11.4	12.7	100.4
P-14B	47.7	1.3	0.3	3.3	20.7	0.9	1.3	0.3	12.6	10.6	99.0
P-14D	48.1	0.8	0.1	1.2	21.5	1.1	1.3	0.3	11.3	9.1	94.8
R-01F	47.0	1.1	0.1	2.0	17.5	2.2	1.7	0.4	11.7	15.3	99.0
R-03B	52.0	4.4	0.7	4.2	8.7	1.7	2.2	1.2	10.1	12.8	98.0
R-05G	50.5	2.5	0.0	1.1	16.1	1.5	2.2	0.9	10.6	14.0	99.4
R-06B	51.7	2.4	0.0	1.3	13.8	1.3	2.1	0.7	10.5	15.1	98.9
R-22	51.4	0.8	0.1	0.6	21.1	1.3	1.7	0.4	10.4	14.3	102.1

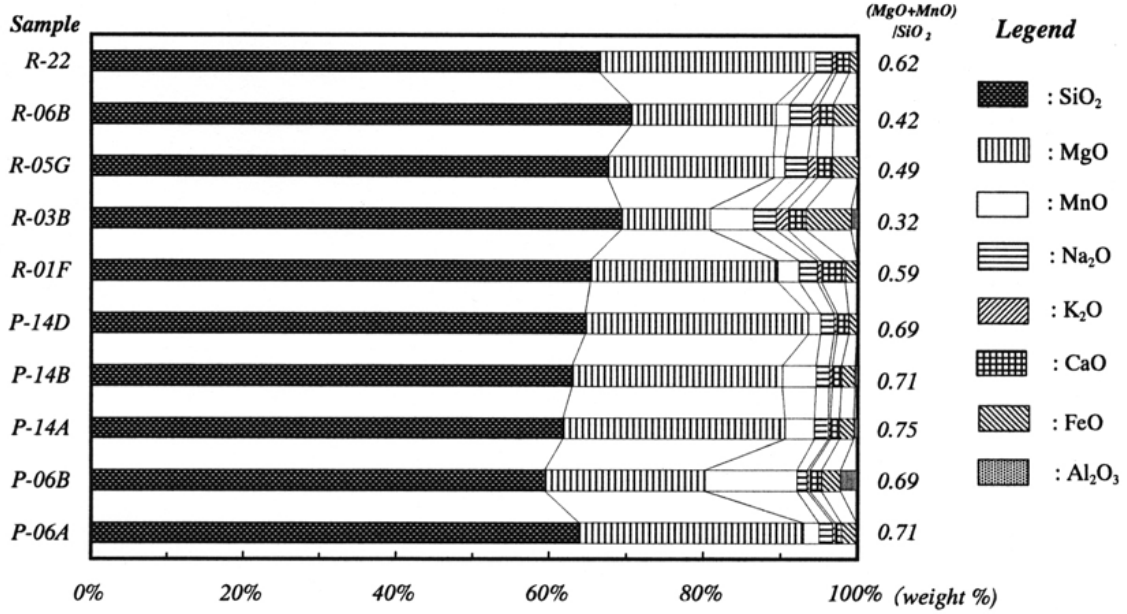

Fig. 2 Distribution of chemical component and (MgO+MnO)/SiO_2 mole ratio of smectite scales collected at the Mori geothermal power plant.

Table 3. Structural formula of scale sample.

sample No.	calculated structural formula
P-06A	$(Na_{0.21}Ca_{0.05}K_{0.03})(Mg_{2.67}Mn_{0.10}Al_{0.06}Fe_{0.01})(Si_{3.92}Al_{0.08})O_{10}(OH)_2 \cdot nH_2O$
P-06B	$(Na_{0.17}Ca_{0.10}K_{0.03})(Mg_{2.02}Mn_{0.66}Al_{0.05}Fe_{0.01})(Si_{3.86}Al_{0.14})O_{10}(OH)_2 \cdot nH_2O$
P-14A	$(Na_{0.22}Ca_{0.08}K_{0.02})(Mg_{2.68}Mn_{0.20}Fe_{0.03})(Si_{3.85}Al_{0.15})O_{10}(OH)_2 \cdot nH_2O$
P-14B	$(Na_{0.21}Ca_{0.08}K_{0.03})(Mg_{2.53}Mn_{0.23}Al_{0.04}Fe_{0.02})(Si_{3.91}Al_{0.09})O_{10}(OH)_2 \cdot nH_2O$
P-14D	$(Na_{0.21}Ca_{0.10}K_{0.03})(Mg_{2.64}Mn_{0.08}Al_{0.04}Fe_{0.01})(Si_{3.96}Al_{0.04})O_{10}(OH)_2 \cdot nH_2O$

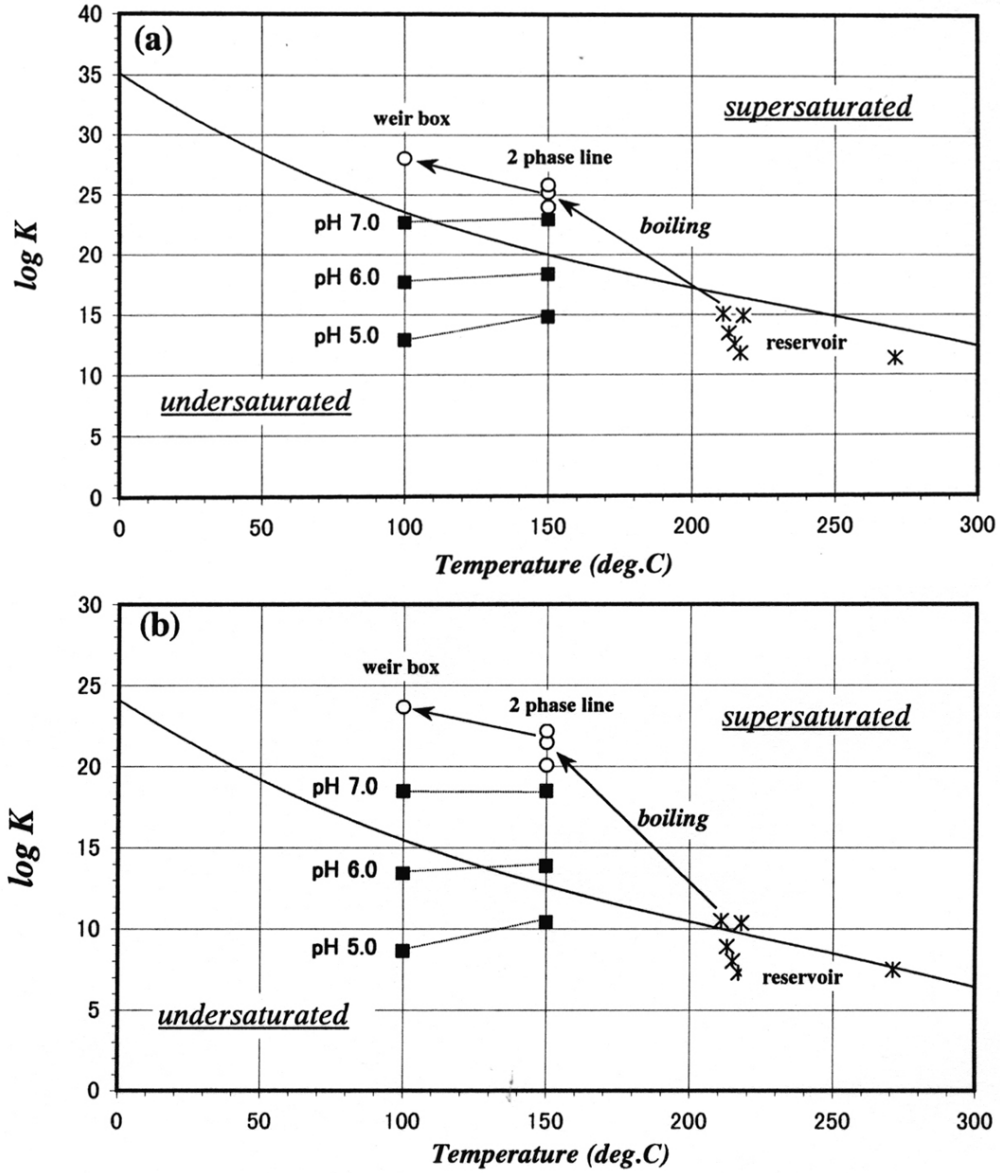

Fig. 3 Solubility of chrysotile (a) and talc (b) in the Mori geothermal fluids and results simulated changing pH to 7.0, 6.0 and 5.0.

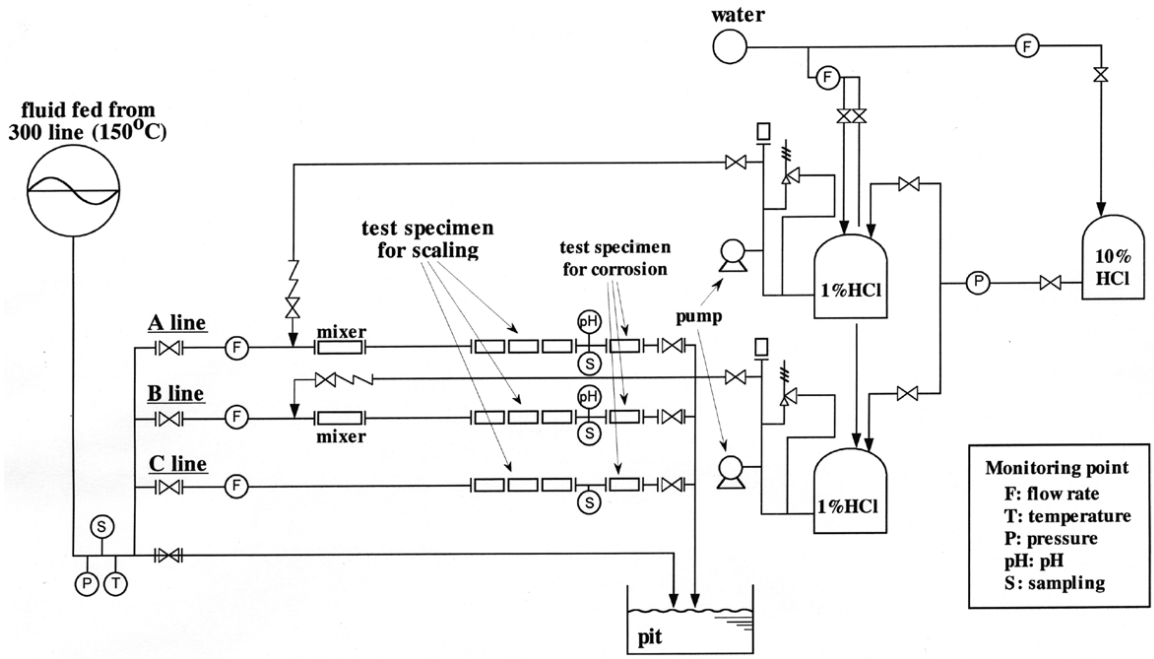

Fig. 4 Diagram of the test plant for scale inhibition by pH control.

Table 4. Results of field test for scale inhibition by pH control.

pH condition	Period (days)	pH monitored	Flow rate (ton/hr)	Weight gain (g)	Deposition rate (g/day)
natural	28	———	2.29±0.11	38.4	1.4
	56	———	2.29±0.16	98.1	1.8
7.0	28	6.97±0.13	2.33±0.07	21.1	0.75
6.5	28	6.47±0.11	2.12±0.42	<0.1	———
	63	6.53±0.10	1.92±0.16	<0.1	———
	87	6.53±0.11	1.67±0.13	<0.1	———
6.0	28	6.03±0.11	2.24±0.13	<0.1	———
	63	6.04±0.10	2.30±0.17	<0.1	———
	87	6.06±0.12	2.31±0.20	<0.1	———
5.0	28	5.05±0.23	2.29±0.11	<0.1	———

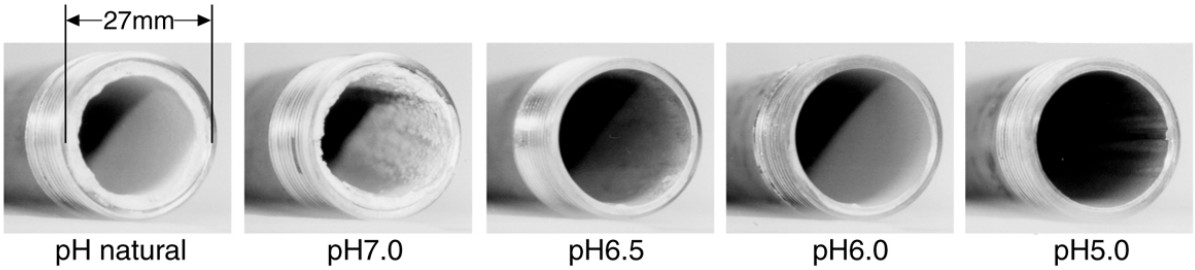

Fig. 5 Specimens of pH control test after 28 days.